FROM PHASE TRANSITIONS TO CHAOS

Edited by
Géza Györgyi
Imre Kondor
László Sasvári
Tamás Tél

World Scientific

Publisher: learn how customers can search inside this book.

Tell the Publisher!
I'd like to read this book on Kindle

Don't have a Kindle? Get yours here.

From Phase Transitions to Chaos: Topics in Modern Statistical Physics (Hardcover)

by G. Gyorgyi (Author), I. Kondor (Author), L. Sasvari (Author), T. Tel (Editor)

No customer reviews yet. Be the first.

List Price: $137.00

Price: **$137.00** & this item ships for **FREE with Super Saver Shipping**. Details

In Stock.

Ships from and sold by **Amazon.com**. Gift-wrap available.

Only 1 left in stock--order soon (more on the way).

Want it delivered Monday, August 3? Order it in the next 15 hours and 3 minutes, and choose **One-Day Shipping** at checkout. Details

2 used from $116.45

Get Free Two-Day Shipping
Get Free Two-Day Shipping for three months with a special extended free trial of Amazon Prime. Add this eligible textbook to your cart to qualify. Sign up at checkout. See details.

Quantity: 1

Add to Shopping Cart

or

Sign in to turn on 1-Click ordering.

or

Add to Cart with FREE Two-Day Shipping

Amazon Prime Free Trial required. Sign up when you check out. Learn More

Add to Wish List

More Buying Choices

3 used & new from $116.45

Have one to sell? Sell yours here

Share with Friends

Editorial Reviews

Product Description

This volume comprises about 40 research papers and essays covering a wide range of subjects in the forefront of contemporary statistical physics. The contributors are scientists and specialists in several different fields. The book is dedicated to Peter Szepfalusy on the occasion of his 60th birthday. Emphasis is placed on his two main areas of research, namely phase transitions and chaotic dynamical systems. They share common aspects like the applicability of the probabilistic approach or scaling behaviour and universality. Several papers deal with equilibrium phase transitions, critical dynamics, and pattern formation. Also represented are disordered systems, random field systems, growth processes, and neural networks. Statistical properties of interacting electron gases, such as the Kondo lattice, the Wigner crystal, and the Hubbard model, are treated. In the field of chaos, Hamiltonian transport and resonances, strange attractors, multifractal characteristics of chaos, and the effect of weak perturbations are discussed. A separate section is devoted to selected mathematical aspects of dynamical systems like the foundation of statistical mechanics, including the problem of ergodicity, and rigorous results on quantum chaos.

Product Details

Hardcover: 585 pages

Publisher: World Scientific Publishing Company (May 1992)

Language: English

ISBN-10: 981020938X

ISBN-13: 978-9810209384

Product Dimensions: 8.9 x 6.1 x 1.2 inches

THE STRUCTURE OF A WEAKLY NONLINEAR RESONANCE

B. V. CHIRIKOV and V. V. VECHESLAVOV
Institute of Nuclear Physics, 630090, Novosibirsk, USSR

ABSTRACT

An example of the weakly nonlinear resonance is considered. The unbounded resonance structure is described in detail, and is shown to be unstable against weak perturbations. Peculiarities of diffusive motion within the intricate chaotic component are discussed.

1. Introduction

The colorful world of nonlinear phenomena, one of whose architects and masters is Professor Péter Szépfalusy, continues to attract an ever growing army of researchers from all the sciences and around. In this paper we hope to put a tiny new touch on this international painting by describing the peculiar phenomenon of the *weakly nonlinear resonance* (WNR). The most striking feature of nonlinear phenomena is the complete rearranging of the motion structure under a weak perturbation. An excellent example is the KAM theory (see, e.g., Ref. 1 and its generalization in Ref. 2) with its subtle, everywhere dense chaotic web.[3,4]

Dynamical chaos—another fascinating discovery in nonlinear mechanics— is almost never just plain disorder but has a highly organized and beautiful structure whose pictures have become common by now on conference advertisements. A new example we are going to discuss below presents one more type of such a structure. This is an intricate interplay of *nonlinear resonances* which control dynamics in Hamiltonian systems.

Let us start with the fundamental Poincaré problem defined by the Hamiltonian

$$H(I,\theta,t) = H_0(I) + \epsilon V(I,\theta,t) \tag{1}$$

where I,θ are N-dimensional action–angle variables, and $\epsilon \to 0$ is a perturbation parameter.

The unperturbed system H_0 is supposed to be 'trivial' that is completely integrable (for good texts in nonlinear dynamics see, e.g., Refs. 1,5). If, in addition, it is nonlinear, that is, the determinant

$$\left| d^2 H_0 / dI^2 \right| \neq 0, \tag{2}$$

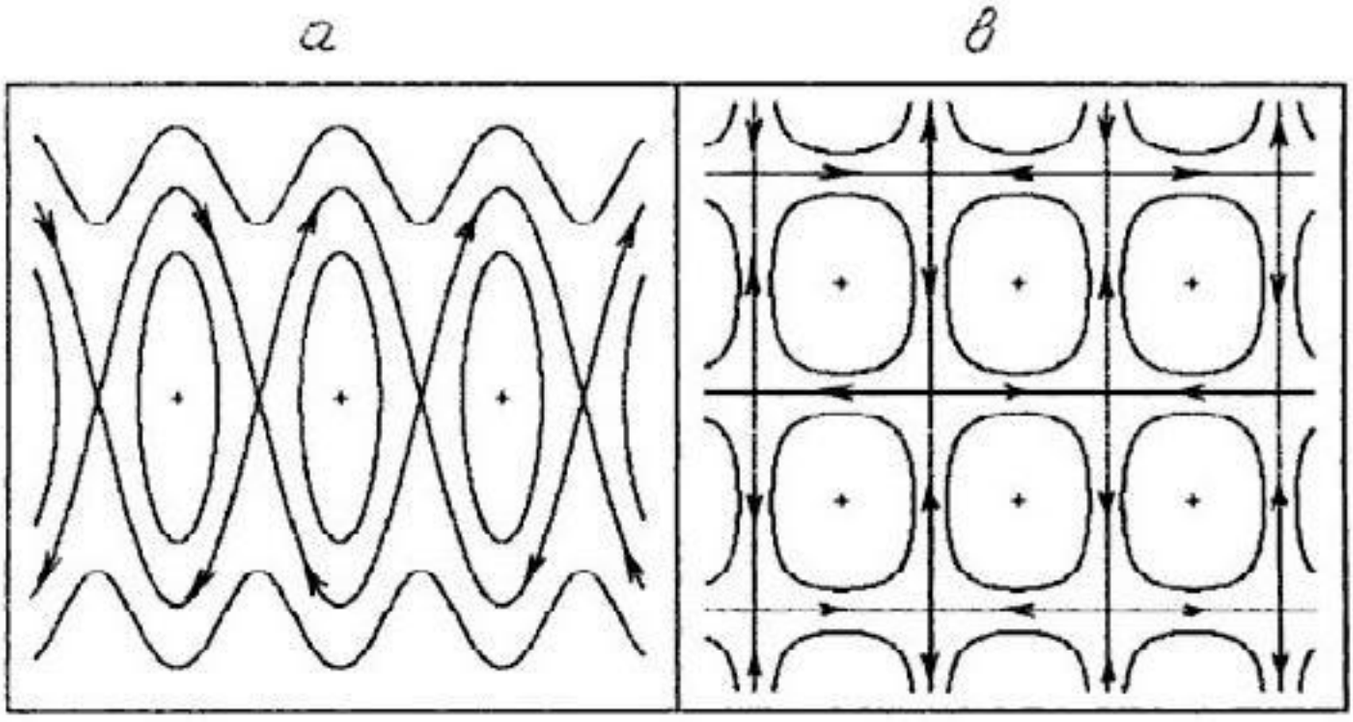

Figure 1: Outline of the resonance phase-space structure for strong nonlinearity (*a*), and for weak nonlinearity (*b*); arrows show the direction of motion.

we call H_0 *strongly nonlinear*. This nonlinearity does not depend on the weak perturbation and remains finite when the latter vanishes.

A single *strongly nonlinear resonance* (SNR) is then also completely integrable and, hence, trivial. Its phase-space picture is now also well known as a 'chain of islands' framed by the separatrix (Fig. 1a) which is the most unstable and chaotic place in the phase space, and which forms the Arnold web mentioned above. This picture is universal and structurally stable, that is, it remains topologically unchanged under sufficiently weak additional Hamiltonian (nondissipative) perturbation. Moreover, the effect of resonant perturbation vanishes with ϵ (e.g., the separatrix swing is $\Delta I \sim \sqrt{\epsilon}$) even though it considerably exceeds that off the resonance ($\Delta I \sim \epsilon$). The *strong nonlinearity suppresses resonant perturbation* if the latter is sufficiently weak. This is one of the principal phenomena in nonlinear Hamiltonian dynamics underlying the celebrated KAM theory.

Remember that for the linear oscillator, that is when the whole Hamiltonian (1) is quadratic in the Cartesian variables p, x, any resonance, internal or driving, produces a big effect, no matter how weak is the perturbation $\epsilon \to 0$. Also, the resonance conditions depend on the oscillator's parameters only, and not on the initial conditions of motion like in the nonlinear oscillator.

Now an interesting question is what happens in between? We call this domain *weak nonlinearity*. In terms of the Hamiltonian (1) it means that the unperturbed Hamiltonian

$$H_0(I) = \omega_0 I \tag{3}$$

is linear in action variables or its frequencies $\omega_0 = \text{const}$, while the perturbation $\epsilon V(I, \theta, t)$ remains arbitrary.

At first glance, this problem may appear simpler than the case of strong nonlinearity, due to another small parameter, nonlinearity $\nu \sim \epsilon$, to which only the perturbation term contributes now. Yet, that is not the case ! A simple explanation is that the weak nonlinearity may not suppress the resonance perturbation whose effect now depends on the ratio ϵ / ν of the two small parameters. In particular, the extension of the KAM theory to weakly nonlinear systems is only possible under the additional requirement of the absence of unperturbed resonances.

Well, physicists are always trying to go ahead of mathematicians. So, consider, on the contrary, the unperturbed resonance! This is certainly a more interesting case. But also a more difficult one. Therefore, we choose a model as simple as possible. One example is given by the Hamiltonian:

$$H(p, x, t) = \frac{p^2 + \omega_0^2 x^2}{2} - \epsilon \cos(x - \Omega t) = \omega_0 I - \epsilon \cos(\rho \cos \theta - \Omega t) \qquad (4)$$

where $\rho = (2 I / \omega_0)^{1/2}$ is the amplitude of the unperturbed oscillations.

This model has been extensively studied in plasma physics where it represents the motion of a charged particle in both the magnetic field (Larmor's frequency ω_0) and the plane wave electric field of strength ϵ (see, e.g., Ref. 5).

If we put $\omega_0 = 0$ the model describes a single SNR ($d^2 H / dp^2 = 1$) which is completely integrable, and so is $H_0(p)$, with no trace of chaos. Moreover, the variation of p is strictly bounded:

$$|\Delta p| \leq 4 \sqrt{\epsilon}. \qquad (5)$$

Yet, for any $\omega_0 \neq 0$ nonlinearity becomes weak (as $\epsilon \to 0$), and the motion drastically changes.

2. The First Order Theory

The first approximation of the conventional resonant perturbation theory[5] for model (4) and related models was thoroughly studied in a series of papers by Sagdeev, Zaslavsky and coworkers (see, e.g., Refs. 6,7, and also Refs. 8–10).

To reveal the resonance structure we first get rid of the unperturbed part $\omega_0 I$ of the Hamiltonian (4) by introducing a new phase $\varphi = \theta - \omega_0 t$, and expanding the perturbation in Bessel functions:

$$\overline{H}(I, \theta, t) = -\epsilon \sum_{k=-\infty}^{\infty} J_k(\rho) \cos\left[k \varphi - (\Omega - k \omega_0) t + \frac{\pi k}{2}\right]. \qquad (6)$$

All terms of this Hamiltonian satisfying $k \lesssim \rho$ are of the same order but differ in the frequency of time-dependence. This difference becomes crucial if we fix a resonance condition: $\Omega = n \omega_0$ with any integer $n \neq 0$ (in the case $n = 0$ the system is

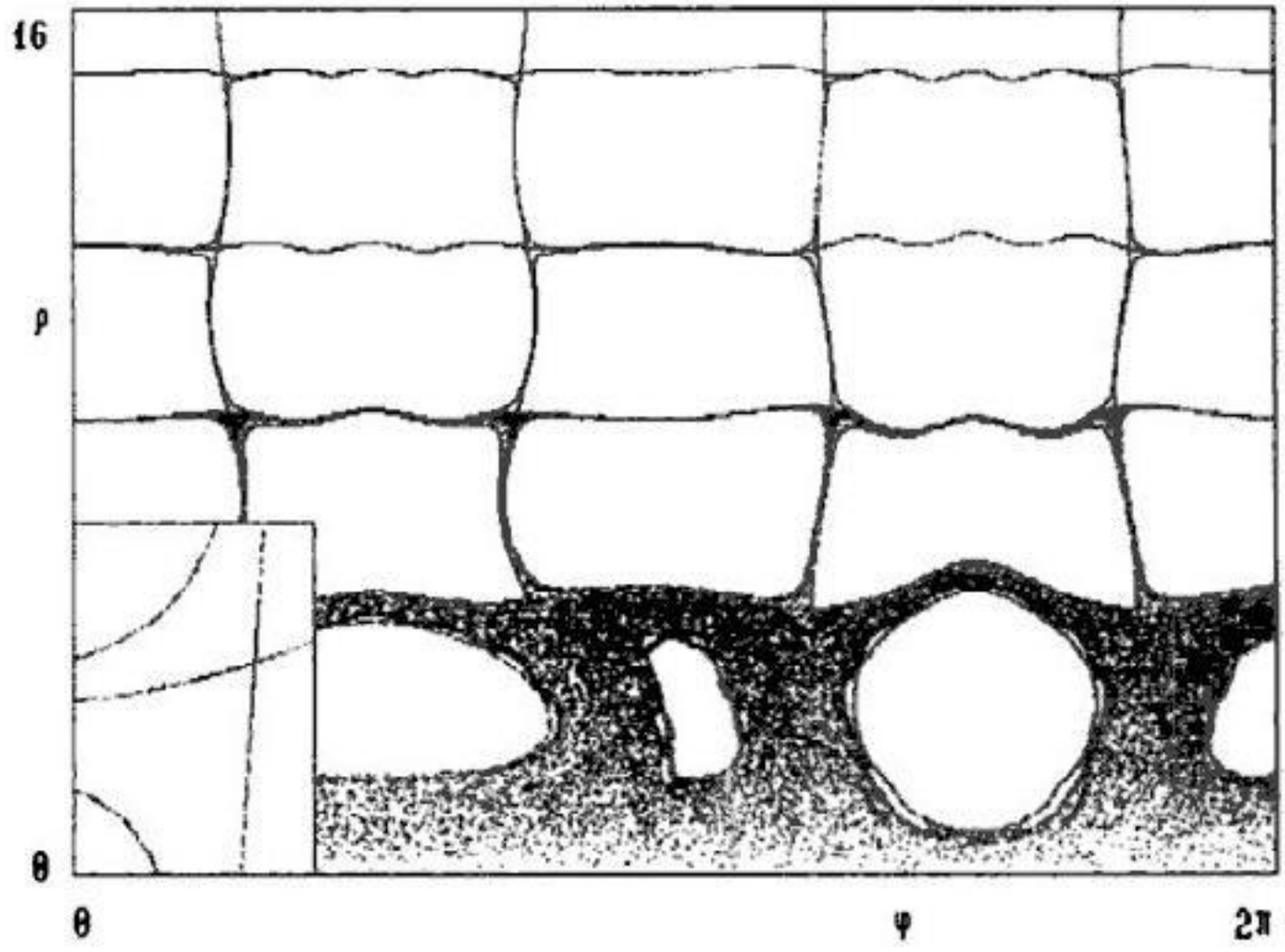

Figure 2: An example of the phase-space structure of a single weakly nonlinear resonance in model (4): $\omega_0 = 1$; $\Omega = 2$; $\epsilon = 1$. Scattered points belong to a single chaotic trajectory bounded by a gap between the third and fourth rows of resonant cells. Inset: an enlarged part of this gap near $\varphi = \pi/4$.

completely integrable). Unlike the linear resonance with only one resonance condition ($\Omega = \omega_0$ for driving perturbation or $\Omega = 2\omega_0$ for parametric one) the WNR is much richer.

Now we can introduce the new unperturbed Hamiltonian

$$\widetilde{H}_0(I, \varphi) = -\epsilon J_n(\rho) \cos\left(n\varphi + \frac{\pi n}{2}\right), \tag{7}$$

the rest of the sum in Eq. 6 being a new perturbation. We emphasize again that the two parts of the new Hamiltonian differ in frequency only, and this difference increases as $\epsilon \to 0$. In other words, the perturbation is no longer small but is a *high-frequency* one (see Eq. 23 below). Hence, the unperturbed motion $\varphi(t)$ is *adiabatic* with respect to the perturbation. We call the whole situation *inverse adiabaticity.*[4]

The most interesting feature is the global structure of the unperturbed motion defined by the Hamiltonian (7) which is outlined in Fig. 1b in coordinates $\Phi =$

$n\varphi + \pi n/2$ and $R = \rho - \pi n/2 - \pi/4$, the latter representing the asymptotics of the Bessel function ($\rho \gg n$)

$$J_n(\rho) \approx \sqrt{\frac{2}{\pi\rho}} \cos R. \tag{8}$$

A real example of this resonance structure, which we are going to discuss in detail below, is presented in Fig. 2. The plane ρ, φ here is Poincaré's surface of section at $t = 0 \bmod 2\pi/\omega_0$, that is, the system's position plotted in each period T_0 of the unperturbed linear oscillation.

This resonance structure is characterized by an infinite(!) lattice of periodic trajectories (fixed points on the plane R, Φ) both stable ($\sin\Phi \approx \sin R \approx 0$) and unstable ($\cos\Phi \approx \cos R \approx 0$), the latter being connected by separatrices. A striking difference from a strongly nonlinear resonance (cf. Fig. 1a)! Instead of a narrow restricted chain of islands we have now the unbounded lattice of resonance cells.

The discovery of this structure was very exciting. It took over 10 years to understand and evaluate the phenomenon. By now(!) it is obvious that the resonance lattice is present in Fig. 2.11 of the monograph by Lichtenberg and Lieberman[5], (see also Refs. 8, 9, cf. Figs. 1b and 2 in this paper). Yet it was missed in both the monograph and its translation into Russian by the present authors! One motivation for this paper is to show that this story is still not over (see Section 3).

Before proceeding let us see how the transition from SNR ($\omega_0 = 0$, Fig. 1a) to WNR (any $\omega_0 \neq 0$, Fig. 1b) takes place. As $\omega_0 \to 0$ is resonant, the parameter $n = \Omega/\omega_0 \to \infty$ (Ω is fixed), and the first zero ρ_1 of $J_n(\rho)$ in Eq. 7 grows indefinitely. The k-th zero has the asymptotic form

$$\rho_k = \frac{\pi n}{2} + \pi k - \frac{\pi}{4}. \tag{9}$$

Thus, the WNR lattice shifts upwards, with the first row of resonance cells $(0, \rho_1)$ expanding indefinitely. For the initial condition inside SNR ($x \sim 1$, $\dot{x} \sim \Omega$, $\rho \sim \Omega/\omega_0 = n$) the coordinate $x \sim \Omega t$ grows with time, as well as ρ, until ρ reaches ρ_1. Around this time the SNR picture completely disintegrates, and only the WNR structure remains.

Already our first numerical experiments with model (4) revealed that the WNR structure is not as simple as it is suggested by Fig. 1b. Besides the distortion of separatrices (a routine perturbation effect) and their chaotic layers (a universal nonlinear phenomenon, see Section 4) we noticed an intricate structure at the intersections of separatrices (see inset in Fig. 2). Further studies showed that the resonance lattice is not a connected formation but is cut through by many narrow gaps.

3. Instability of the Resonance Lattice

Unlike the SNR chain, the WNR lattice proved to be structurally unstable. We shall analyze this problem using the asymptotic representation (8) of the unperturbed

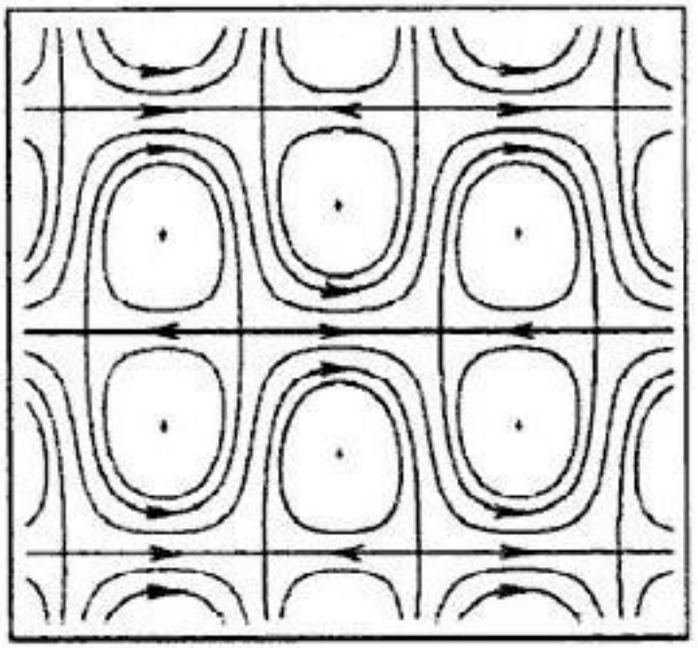

Figure 3: A scheme of WNR structure with perturbation (12) for $\beta = 0$ (cf. Fig. 1b); the separation of resonance cell rows by horizontal gaps is clearly seen.

Hamiltonian (7),

$$\widetilde{H}_0(I,\varphi) = -\epsilon\sqrt{\frac{2}{\pi\rho}}\cos R\cos\Phi + V(I,\varphi), \tag{10}$$

where we have introduced the additional time-independent perturbation V. Remember that we are studying the stability of the unperturbed WNR structure. The impact of the high-frequency perturbation will be considered later (Section 4).

Introducing new time and dynamical variables

$$\tau = t\epsilon\sqrt{\frac{2}{\pi\rho}} \qquad (\rho \approx \text{const}),$$

$$r = R - R_k, \qquad s = \Phi - \Phi_k, \tag{11}$$

and keeping for the perturbation V only terms linear in the new variables, we arrive at the new Hamiltonian

$$\widetilde{H}_0(I,\varphi) = -\sin r\sin s + \alpha r + \beta s. \tag{12}$$

Here R_k,Φ_k are the coordinates of a certain fixed point (see Fig. 1b), and the canonical variables remain I,φ as before.

Consider first a simpler case $\beta = 0$ (for $\alpha, \beta \neq 0$ see Section 7). Then the horizontal separatrices ($r = \text{const}$) all remain unchanged, but the vertical ones ($s = \text{const}$) are destroyed because of the difference in $\widetilde{H}_0$ between the two neighbouring

fixed points ($\Delta\widetilde{H}_0 = \pi\,|\alpha|$). The new structure is outlined in Fig. 3. Remarkably, an arbitrarily small perturbation ($\alpha \to 0$) qualitatively changes the structure making all the rows of resonance cells disconnected by narrow horizontal gaps. For small $\alpha > 0$ the width of a gap at $s = \pi/2$ and $r = 0 \bmod 2\pi$ is:

$$\Delta\rho \approx 2\left|\frac{\Delta\widetilde{H}_0}{\partial\widetilde{H}_0/\partial r}\right| \approx 2\pi\,|\alpha|. \tag{13}$$

Actually, each of these gaps consists of two nearly equal parts at both sides of the horizontal separatrix. The position of a gap in s is determined by the condition:

$$\alpha\cos r\sin s < 0 \quad or \quad \alpha\dot{\varphi} > 0. \tag{14}$$

Particularly, for a given α the direction of motion is the same in all gaps.

The perturbation shifts the fixed points whose position is determined by the equations:

$$\cos r\sin s - \alpha = 0, \qquad \sin r\cos s = 0, \tag{15}$$

with two solutions

$$\begin{aligned} \cos s_1 &= 0, \qquad \cos r_1 = \pm\alpha, \\ \sin s_2 &= \pm\alpha, \qquad \sin r_2 = 0, \end{aligned} \tag{16}$$

for stable and unstable fixed points, respectively. If

$$|\alpha| > 1, \tag{17}$$

the WNR structure is completely destroyed, and all the gaps unite.

Consider, as an example, the model with Hamiltonian [7,11]

$$H(p,x,t) = \frac{p^2}{2} - \cos(\omega_0 x) - \epsilon\cos(x - \Omega t). \tag{18}$$

Globally, this model describes the interaction of the two SNRs which results in the formation of relatively narrow chaotic layers around resonance separatrices. But near the center of the stronger resonance ($x \approx 0$) the model (18) is close to our basic model (4) of WNR. If $\Omega \neq n\omega_0$ the resonance center is stable for $\epsilon \to 0$. But for $\Omega = n\omega_0$ a WNR lattice is formed inside the SNR. However, the former is destroyed at sufficiently large x as the nonlinearity in Eq. 18 is strong. For $|\omega_0 x| \ll 1$ the nonlinearity is described by the term

$$\delta H = \frac{\omega_0^4}{24}\langle x^4\rangle = \frac{\omega_0^4\rho^4}{64}. \tag{19}$$

Linearizing this nonlinear perturbation in ρ we arrive, for $\rho \gtrsim n$, at Hamiltonian (12) with $\beta = 0$ and

$$\alpha = \sqrt{\frac{\pi}{2}}\,\frac{\omega_0^4\,\rho^{7/2}}{16\,\epsilon} = 1. \tag{20}$$

The latter equality determines the border between the WNR structure (with gaps, $\alpha < 1$) and the SNR behavior ($\alpha > 1$). Particularly, the size ρ_w of the former is given by the relation

$$\frac{\rho_w}{\rho_s} = 0.66 \left(\frac{\epsilon}{\omega_0^4}\right)^{2/7}. \tag{21}$$

where $\rho_s = \pi/\omega_0$ is the SNR separatrix size in x. This estimate holds in the interval

$$n \lesssim \rho_w \lesssim 1/\omega_0, \tag{22}$$

provided (see Eqs. 6,7)

$$\left|\frac{n\dot{\varphi}}{\omega_0}\right| \equiv \frac{1}{\lambda} = \sqrt{\frac{2}{\pi}} \frac{\epsilon n}{\omega_0^2 \rho^{3/2}} \lesssim 1. \tag{23}$$

This adiabaticity parameter is going to play an important role in what follows (see Section 4). At the border $\rho = \rho_w$ (see Eq. 21)

$$\lambda_w^{-1} \sim \Omega \epsilon^{4/7} \omega_0^{3/14} \to 0$$

as $\omega_0 \to 0$ with fixed Ω and ϵ. The inequalities (22) imply that $\Omega \lesssim 1$.

Comparison with numerical results in Refs. 11,7 shows that the accuracy of Eq. 23 is about 10 per cent even for $\rho_w/n \approx 1.5$.

The unbounded WNR lattice is related to the periodicity in ρ of the unperturbed Hamiltonian (7) due to the special structure of the perturbation in Eq. 4. Again, unlike the SNR behavior the WNR one is not universal. For example, if the additional nonlinear term (19) were proportional to ϵ, i.e., weakly nonlinear according to our definition above, then the parameter α would be independent of ϵ, while the resonance structure would vary in a broad range, from WNR ($\omega_0 \to 0$) to SNR ($\omega_0 \to \infty$).

Another simple example is a detuning $\delta\Omega = n\,\delta\omega_0$ from the resonance $\Omega = n\omega_0$. The additional term in Hamiltonian (4) is $\delta H = \omega_0\,\delta\omega_0\,\rho^2/2$, hence the perturbation parameter

$$\alpha = \sqrt{\frac{\pi}{2}} \frac{\omega_0 \rho^{3/2}}{\epsilon} \delta\omega_0 = \lambda \frac{\delta\Omega}{\omega_0} \tag{24}$$

is in agreement with the previous result in Ref. 8. Notice that for a fixed $\delta\Omega \neq 0$ the WNR structure is always destroyed as $\lambda \to \infty$ ($\epsilon \to 0$). This is a simple explanation of the KAM integrability for weak nonlinearity.

Coming back to model (4) we wonder what may be the origin of the gaps revealed in our numerical experiments ? Apparently, it is the effect of a higher-order perturbation, namely, the second-order correction to the unperturbed Hamiltonian (7). It can be evaluated as follows.

First, we rewrite the original Hamiltonian (4) in the form ($\omega_0 = 1$, $\Omega = n$)

$$H(I, \theta, t) = I - \epsilon \cos(\rho \cos\theta) + \epsilon\,[\cos(\rho \cos\theta) - \cos(\rho \cos\theta - nt)]\,. \tag{25}$$

We expand it in Bessel functions, then change variables $I, \theta \to I_1, \theta_1$ so as to eliminate all first-order terms in the brackets but the resonant one (7). Finally, we introduce a new phase $\varphi_1 = \theta_1 - t$. As it can be verified easily, the time-independed part of the result is given up to terms $\sim \epsilon^2$ by the expression

$$\widetilde{H}_0(I,\varphi) = -\epsilon J_n(\rho)\cos\left(n\varphi + \frac{\pi n}{2}\right) + \frac{\epsilon^2}{\rho}\sum_{m\geq 1}\frac{d}{d\rho}J^2{}_{2m}(\rho) - \frac{\epsilon^2}{\rho}\sum_{m\neq n}\frac{m}{m-n}\frac{d}{d\rho}J^2{}_m(\rho) \tag{26}$$

where we dropped the subscript 1. Asymptotically, the second sum can be neglected for it decreases faster ($\sim \rho^{-1}$) than the first one,

$$\sum_{m\geq 1}\frac{d}{d\rho}J^2{}_{2m}(\rho) = -\frac{1}{2}\left[J_1(2\rho) - 2J_1(\rho)J_0(\rho)\right] \to -\frac{1}{2\sqrt{\pi\rho}}\cos\left(2\rho - \frac{3\pi}{4}\right). \tag{27}$$

On all horizontal separatrices (Fig. 1b) $\cos(2\rho_k - 3\pi/4) \approx \cos(\pi n + \pi/4) = (-1)^{n+1}/\sqrt{2}$ is approximately the same, and we arrive at Hamiltonian (12) with

$$\alpha = -\frac{3}{8}(-1)^n\frac{\epsilon}{\rho_k{}^2}. \tag{28}$$

From Eq. 13 the gap width is

$$\Delta\rho_k = \frac{3\pi}{4}\frac{\epsilon}{\rho_k{}^2}. \tag{29}$$

4. Chaotic Web

Without the high-frequency perturbation (see Eq. 6), all separatrices are lines on the surface of section ρ, φ and all rows of resonance cells are separated by the gaps. As is well known, the perturbation destroys separatrices and produces chaotic layers. If the width of a layer exceeds that of the adjacent gap the rows get connected and the global motion drastically changes.

The unperturbed motion on a separatrix can be found from the first-order Hamiltonian (7), and, for a horizontal ($\rho \approx$ const) separatrix, is described by the equation

$$\dot{\Phi}_s = \frac{\omega_0}{\lambda}\cos\Phi_s. \tag{30}$$

The solution

$$\frac{\omega_0 t}{\lambda} = \ln\tan\left(\frac{\Phi_s}{2} + \frac{\pi}{4}\right) \tag{31}$$

is the same as for the SNR separatrix. Hence, the well developed theory of the chaotic layer (see, e.g., Ref. 3) is applicable. Particularly, the amplitude of the variation of the Hamiltonian (7) , or separatrix splitting, is given by the relation

$$\Delta H_s = \epsilon J_k(\rho)\int_{-\infty}^{\infty}\cos(k\varphi(t) + \omega_0 t)\,\omega_0\,dt$$

$$= \epsilon J_k(\rho) \int_{-\infty}^{\infty} \cos(m\Phi + \omega_0 t)\,\omega_0\,dt \approx 2\pi\epsilon J_k(\rho)\frac{(2\lambda)^m}{\Gamma(m)}\exp(-\pi\lambda/2), \qquad (32)$$

where $\Gamma(m)$ is the gamma-function and the latter expression holds for $\lambda \gg 1$. Notice that the effect is exponentially small in λ which is characteristic for adiabatic processes.

Of all perturbation terms in the Hamiltonian (6) only two with the lowest frequencies are operative with the corresponding values of the parameter m

$$k = n \pm 1, \qquad m = \frac{n \pm 1}{n}. \qquad (33)$$

Of these two the main contribution comes from the one for which $\dot{\varphi}(n-k) > 0$. Taking account of Eqs. 14 and 28 we have

$$m = \frac{n+1}{n}, \quad n \text{ even}; \qquad m = \frac{n-1}{n}, \quad n \text{ odd}. \qquad (34)$$

In the first case the chaotic layer is considerably wider than in the second (see Eq. 32). We mention that our result is somewhat different from that in Refs. 6,7.

As $\lambda \sim \rho^{3/2}$, the nonadiabatic effect, Eq. 32, exponentially decreases with the growth of ρ by a factor of

$$g = \exp\left(-\frac{3\pi^2}{4}\frac{\lambda}{\rho}\right) \ll 1 \qquad (35)$$

for each period $\Delta\rho = \pi$ of the resonance lattice. Particularly, this implies that in evaluating ΔH_a the minimal ρ should be taken within a connected chaotic layer. For the upper half of a gap (see Fig. 3) it is $\rho = \rho_g$, but for the lower part $\rho = \rho_g - \pi$. As a result, the latter is closed at a smaller perturbation.

Another interesting implication is the competition of the two mechanisms of closing the upper half of the gap. One is related to the width of its chaotic layer

$$\Delta H_s = \lambda \Delta H_a, \qquad (36)$$

taken at $\rho = \rho_g$. The second one corresponds to a single change ΔH_a but taken at a smaller $\rho = \rho_g - \pi$. Their ratio

$$\frac{\Delta H_s(\rho_s)}{\Delta H_a(\rho_g - \pi)} \approx \lambda g \qquad (37)$$

asymptotically drops with ρ. Thus, for sufficiently large ρ the second mechanism is decisive.

Using Eqs. 29, 32 and the relation $|\Delta H_a| = \Delta\rho_a \left|d\widetilde{H}_0/d\rho\right| \approx \Delta\rho_a\,\epsilon J_n(\rho)$ we obtain for the ratio ($\omega_0 = 1$)

$$\frac{\Delta\rho_a}{\Delta\rho_k} \approx \frac{4}{3\Gamma(m)}\left(\frac{4}{\pi}\right)^m n\sqrt{\rho_g}\Lambda^{m+1}(\rho_g)\exp[-\Lambda'(\rho_g)], \qquad (38)$$

where the new symbols are

$$\Lambda(\rho_g) = \frac{\pi}{2}\lambda(\rho_g) \approx \frac{2{\rho_g}^{3/2}}{\epsilon n}, \qquad \Lambda'(\rho_g) = \Lambda(\rho_g - \pi). \tag{39}$$

The second one is the main (but not the only) parameter related to the closing of the gap which roughly corresponds to $\Delta\rho_a \approx \Delta\rho_k$.

5. Numerical Experiments

The gaps discussed above are typically very narrow, and this was apparently the reason why they were missed in previous studies.[6,7] Also, to compute the width of a gap and check relation (29) a high accuracy of computation is required. Instead of the time-dependent Hamiltonian (4) we made use of the equivalent model

$$H(I, K, \theta, \psi) = I + nK - \epsilon\cos[x(\theta, I) - \psi] = \text{const}, \tag{40}$$

where we put $\omega_0 = 1$; $\Omega = n$. This Hamiltonian is conserved which allows the efficient control of computation errors. The equations of motion were represented as a third-order implicit map which provided exact conservation of the phase-space volume.[12]

At first, the width of the gaps were measured for several values of ρ_k ($J_n(\rho_k) = 0$, $n = 2$, $\varphi = 0$, $8.5 \le \rho_k \le 49.5$) and sufficiently weak perturbation strength ϵ when the chaotic layers could be neglected. The top and bottom borders of the gap were located by identifying the transition of the border trajectory from rotation to oscillation, or vice versa, during one period of slow motion. In all computations the time-step was choosen so that the conservation of Hamiltonian (40) is better than 10 per cent of its variation over the gap.

If the perturbation parameter ϵ increases, the chaotic layer occupies some part of the gap, and, finally, closes the gap completely. We studied this process by running 16 trajectories equidistributed across the gap for a hundred of slow motion periods. The number of trajectories which persisted in the gap and did not deviate into the adjacent chaotic layers determined the remaining width of the gap $\Delta\rho_r$.

Our main numerical results are represented in Fig. 4 by diamonds for 23 gaps with different ρ and ϵ ($8.5 \le \rho \le 49.5$; $0.5 \le \epsilon \le 7$). This figure shows the dependence $\Delta\tilde{\rho}(\Lambda)$ where

$$\Delta\tilde{\rho} = \frac{\Delta\rho_r}{\Delta\rho_k} = \frac{\Delta\rho_r {\rho_k}^2}{(3\pi/4)\epsilon} \tag{41}$$

is the ratio between the actual gap width $\Delta\rho_r$ and the asymptotic value (29) without chaotic layers, which depend on the parameter $\Lambda = {\rho_k}^{3/2}/\epsilon$ (see Eq. 38). For large Λ values the chaotic layers can be neglected, and $\Delta\tilde{\rho} \to 1$ as expected. Higher values of $\Delta\tilde{\rho}$ for smaller Λ are apparently due to deviations from asymptotical dependence

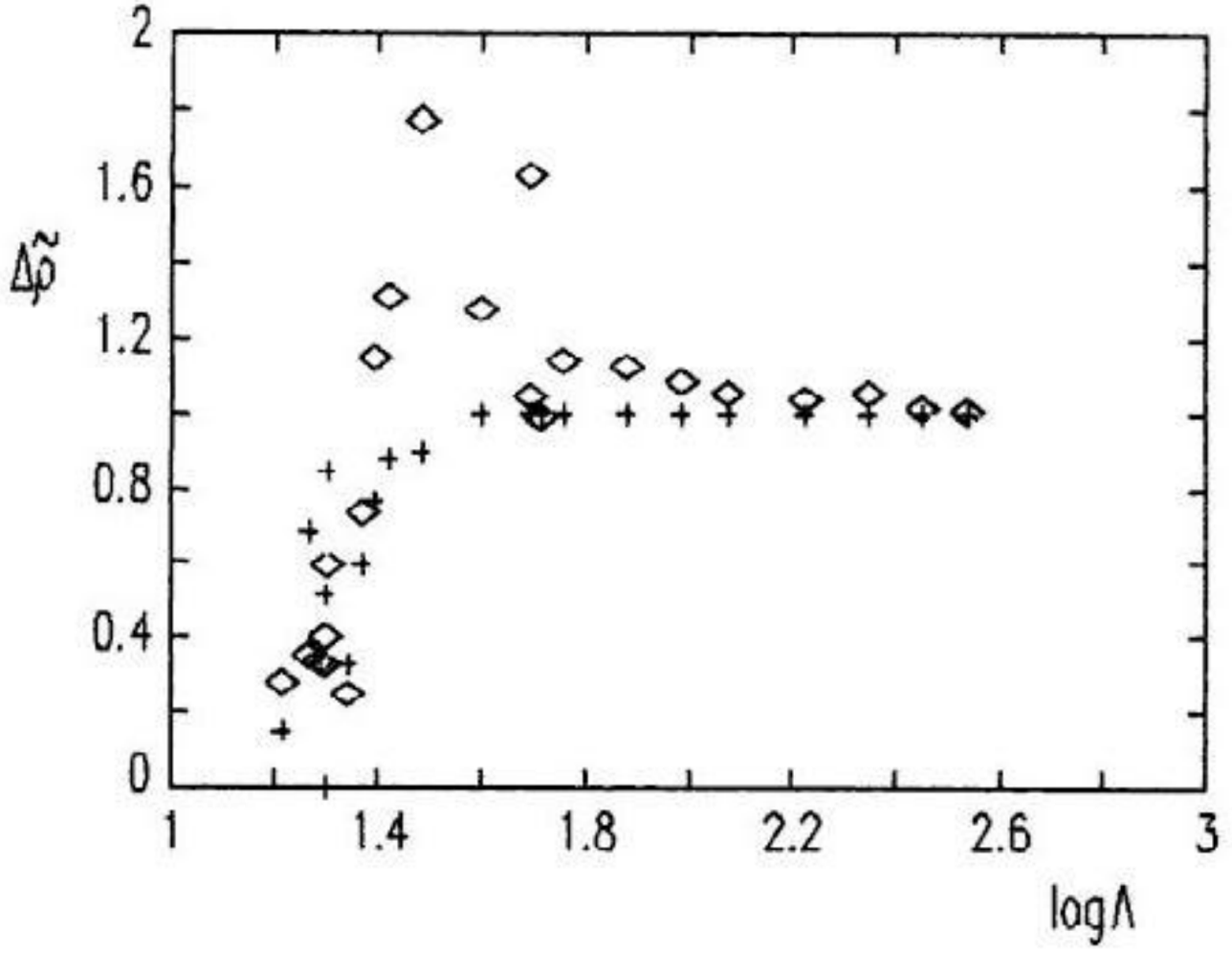

Figure 4: The dependence of the reduced gap width $\Delta\tilde{\rho}$, Eq. 41, on the chaotic layer parameter Λ, Eq. 39: diamonds are numerical results, crosses are theoretical estimates (Eq. 42). Logarithm is decimal.

(29). The sharp cut-off in $\Delta\tilde{\rho}(\Lambda)$ at $\Lambda \approx 20$ is the effect of chaotic layers which close the gaps. This effect can be estimated using Eq. 38 as

$$\Delta\tilde{\rho} \approx 1 - \frac{\Delta\rho_a}{\Delta\rho_k} \approx 4.3\sqrt{\rho_k}\Lambda^{5/2}\exp(-\gamma\Lambda'), \qquad (42)$$

where we put the values $n = 2$, $m = 3/2$ used in the numerical experiments. The theoretical values of $\Delta\tilde{\rho}$ are also plotted in Fig. 4 by small crosses. Notice the scattering of the latter which is explained by the dependence of $\Delta\tilde{\rho}$ on the two different variables, ρ_k and ϵ.

The deviation from the theoretical estimate (38) is apparently related to the poor approximation (30) where the unperturbed separatrix is used. By introducing the fitting parameter $\gamma \approx 0.78$ good agreement between numerical and theoretical values of $\Delta\tilde{\rho}$ can be achieved, which seems to be satisfactory for such a delicate phenomenon as the separatrix chaotic layer.

6. Diffusion Peculiarities in Resonance Web

Now we are going to compare the motion within the WNR web and the Arnold diffusion (AD) in a strongly nonlinear system. One thing in common is the network of chaotic layers of a similar structure as we have seen in Section 4. An important difference is the minimal dimensionality to permit diffusion: $N = 2$ degrees of freedom for WNR web and $N = 3$ for AD (in conservative systems). Also, the former is not universal, in contrast to AD. First, the WNR structure itself is not universal as discussed above (see Section 3), and second, even such a WNR web is structurally unstable (Section 3) so that the diffusion is restricted by the gaps.

Furthermore, within the allowed region the WNR diffusion is very peculiar. The local diffusion rate averaged over many resonance cells (not a good approximation because of a small factor $g \ll 1$, Eq. 35, see below) is according to Refs. 4,13

$$D_p \equiv \frac{\langle(\Delta p)^2\rangle}{t} \approx \frac{\omega_0}{\pi\lambda^3} \sim \frac{\epsilon^3 n^3}{\omega_0^5 \rho^{9/2}}, \tag{43}$$

that is very fast compared to AD which is exponentially small in λ. This is because in the present case the diffusion proceeds in big jumps ($\Delta p = \pi$) instead of $\Delta p \sim \exp(-\pi\lambda/2)$ for AD. Yet, it does not mean that the global diffusion is always fast.[6,7,9] The point is that the general Fokker-Planck-Kolmogorov diffusion equation has two terms[5]

$$\frac{\partial f(p,t)}{\partial t} = \frac{1}{2}\frac{\partial}{\partial p} D_p(p) \frac{\partial f}{\partial p} - \frac{\partial}{\partial p} B_p(p) f, \tag{44}$$

the second one describing the drift

$$V_p(p) \equiv \frac{\langle p\rangle}{t} = B_p + \frac{dD_p}{dp}. \tag{45}$$

Function $B_p(p)$ can be derived from Einstein's relation using the steady-state distribution, or invariant measure

$$f_s \sim \exp(-\pi\lambda/2), \tag{46}$$

which is roughly proportional to the chaotic layer's width (36). From Eqs. 44, 45 we have

$$B_p = \frac{D_p}{2}\frac{d\ln f_s}{dp} \sim -\frac{\epsilon^2 n^2}{\omega_0^3 \rho^4},$$

$$V_p \sim -\frac{\epsilon^3 n^3}{\omega_0^5 \rho^{11/2}} - \frac{\epsilon^2 n^2}{\omega_0^3 \rho^4} \sim -\frac{\epsilon^2 n^2}{\omega_0^3 \rho^4}. \tag{47}$$

Term B_p in Eq. 45 dominates, since the ratio

$$\frac{dD_p/dp}{B_p} \sim \frac{1}{\lambda} \ll 1. \tag{48}$$

The drift acts as a damping even though the system is Hamiltonian. This is a peculiar effect of the specific structure of the chaotic component. Notice that if its measure $f_s(\rho)$ grew with ρ, a blow-up would occur ($V_\rho > 0$) instead of damping.

In any case, the diffusion is fast but in one direction only, downwards in our case. The average motion in this direction becomes dynamical (the 'secondary dynamics' we usually say) described by the equation

$$\frac{d\rho}{dt} \approx V_\rho(\rho) \approx -C\frac{\epsilon^2 n^2}{\omega_0^3 \rho^4} \ , \tag{49}$$

where $C \sim 1$ is a constant. Particularly, the 'fall' time is

$$t_f \approx \frac{\omega_0^3 \rho_0^5}{5C\epsilon^2 n^2}, \tag{50}$$

where ρ_0 is the initial value.

A better approximation for t_f is simply to sum up the life times at each row (see Eq. 43)

$$t_f \approx \sum_{k=1}^{k_0} \frac{\pi^2}{D_\rho} \approx C_1 \int_0^{\rho_0} \frac{\omega_0^5}{\epsilon^3 n^3} \rho^{9/2}\, d\rho = \frac{2C_1}{11}\frac{\omega_0^5}{\epsilon^3 n^3}\rho_0^{11/2}, \tag{51}$$

where $C_1 \sim 1$ is some constant and k_0 stands for the initial value.

The motion upwards, forbidden in dynamical approximation, is only possible due to statistical fluctuations of a chaotic trajectory. A crude estimate for the 'ascension' time t_a can be obtained from the statistical balance of transitions between the lower part of the steady state with measure $\mu_0 \approx 1$ and an upper part ($\rho > \rho_1$) of a small measure $\mu_1 = f_s \sim exp(-\pi\lambda/2)$ (see Eq. 46)

$$\frac{\mu_0}{t_a} \sim \frac{\mu_1}{t_f},$$

whence

$$t_a \sim t_f \exp(\pi\lambda/2). \tag{52}$$

This mechanism of dynamical-statistical transport is also typical for AD in a SNR chaotic web (see, e.g., Refs. 3–5,10). It increases the numerical factor in the exponent for the mean diffusion rate.

7. Linear Resonance in Nonlinear Web

Now we consider the effect of the second perturbation in Hamiltonian (12), that is, the case $\beta \neq 0$. If $\alpha = 0$ the resonance structure simply turns by the angle $\pi/2$ due to the symmetry of Hamiltonian in this approximation. In particular, the gaps become vertical, lying along r rather than along s as before. For the original system this would be a crucial change implying a fast energy growth for the initial conditions

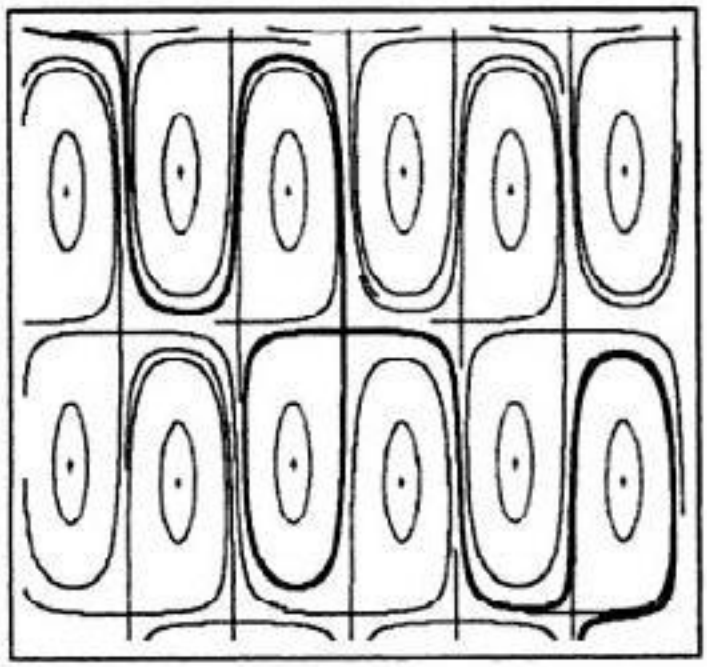

Figure 5: Outline of the WNR structure with perturbation (12) for $\alpha = 0.041$; $\beta = 0.1$. One of the unclosed separatrices is shown by the fat line.

in the gaps if $\beta < 0$ (cf. Eq. 14, the opposite sign is due to canonical conjugation in Hamiltonian systems). Since s is an angle, the perturbation is periodic in φ, and the parameter β has both signs at different φ. The linear approximation (12) makes sense for $n \gg 1$ only.

A more interesting resonance structure arises when both α and β are nonzero. In this case all unperturbed separatrices are destroyed or, better to say, drastically transformed. If $|\alpha|, |\beta| \ll 1$ the fixed points are shifted only slightly but the shape of four separatrices (two ingoing and two outgoing) per unstable fixed point are now completely different. As outlined in Fig. 5 (cf. Figs. 1b and 3) two of them unite and frame a cell of closed trajectories around the stable fixed point while the two remaining (unclosed) determine the gaps. In the infinite lattice in both r and s the unclosed separatrices are also infinite for irrational α/β which is the typical case. For rational α/β the unclosed separatrix ends at some other fixed point.

At average (over many resonance cells) the unclosed separatrices follow the perturbation levels ($\alpha r + \beta s = const$ in linear approximation (12)). The global behavior of gaps is not universal and crucially depends on a particular perturbation. To get an idea what it could be like, we consider the additional perturbation to Hamiltonian (4) in the form

$$\delta H(p, x, t) = \nu\, x \cos \Omega_1 t, \tag{53}$$

which is the linear driving perturbation. It becomes resonant if we put $\Omega_1 = \omega_0$ which is the second resonance in addition to $\Omega = n\omega_0$. With linear perturbation

(53) and second-order term (26) the Hamiltonian (7) becomes

$$\widetilde{H}_0(I,\varphi) = -\epsilon J_n(\rho)\cos\left(n\varphi + \frac{\pi n}{2}\right) + \frac{(-1)^n}{2\sqrt{2\pi}}\frac{\epsilon^2}{\rho^{3/2}} + \frac{\nu\rho}{2}\cos\varphi. \tag{54}$$

As is easily verified the high-frequency term in perturbation (53) results, to order ν^2, in a change of the Hamiltonian which does not affect the motion. The gap trajectories $\rho(\varphi)$ approximately satisfy the conservation law

$$\frac{(-1)^n}{2\sqrt{2\pi}}\frac{\epsilon^2}{\rho^{3/2}} + \frac{\nu\rho}{2}\cos\varphi \approx \text{const}, \tag{55}$$

as explained above.

The analysis of this equation shows that there exists a certain critical value of $\rho = \rho_c$ such that for $\rho > \rho_c$ the gap trajectories go to infinity ($\rho \to \infty$) while below ρ_c their oscillations are bounded. Approximation (55) holds for $\nu \ll \epsilon^2$ only when $\rho \gg 1$, and

$$\rho_c \approx \left(\frac{4\epsilon^2}{27\sqrt{2\pi}|\nu|}\right)^{2/9} \approx 0.53\left(\frac{\epsilon^2}{|\nu|}\right)^{2/9}. \tag{56}$$

In the opposite limit ($\nu \gg \epsilon^2$) all the gap trajectories are apparently unbounded, but this case requires further analysis.

In conclusion we would like to emphasize again the richness of nonlinear dynamics even in fairly simple models as those discussed above.

References

1. V. I. Arnold and A. Avez, *Ergodic Problems of Classical Mechanics* (Benjamin, 1968).
2. N. N. Bogolyubov, Yu. A. Mitropolsky, and A. M. Samoilenko, *Methods of Accelerated Convergence in Nonlinear Mechanics* (Springer,1976).
3. B. V. Chirikov, *Phys. Reports* **52** (1979) 263.
4. B. V. Chirikov and V. V. Vecheslavov, *KAM Integrability*, in *Analysis etc.*, eds. P. Rabinowitz and E. Zehnder (Academic Press, 1990) p.219.
5. A. Lichtenberg and M. Lieberman, *Regular and Stochastic Motion* (Springer, 1983).
6. A. A. Chernikov, R. Z. Sagdeev, and G. M. Zaslavsky, *Physica* **D33** (1988) 65.
7. G. M. Zaslavsky *et al.*, *Weak Chaos and Quasiregular Structures* (Moskva, Nauka, 1991, in Russian).
8. A. V. Timofeev, *Nucl. Fus.* **14** (1974) 165.
9. A. Fukuyama *et al.*, *Phys. Rev. Lett.* **38** (1977) 701.
10. B. V. Chirikov and V. V. Vecheslavov, *How Fast is the Arnold Diffusion?* (Preprint INP 89-72, Novosibirsk, 1989).
11. A. A. Chernikov *et al.*, *Phys. Lett.* **A122** (1987) 39.

12. V. V. Vecheslavov, *Canonical Integration in Any Order* (Preprint INP 89-35, Novosibirsk, 1989, in Russian).
13. A. Lichtenberg and B. Wood, *Diffusion Through a Stochastic Web* (Berkeley, 1988, unpublished).